Model for spatial microtubule oscillations

D. Sept
Department of Chemistry and Biochemistry, University of California, San Diego, La Jolla, California 92093-0365
(Received 21 May 1998; revised manuscript received 27 October 1998)

Under particular *in vitro* conditions, oscillating spatial and temporal waves of assembled microtubules can be observed. A reaction-diffusion model is presented to reproduce these results. This model is based on a set of chemical reaction equations and extended to include spatial dependence and diffusion. The basic properties of the model are presented and the results are demonstrated to connect the observable waves with turbidimetric measurements. The results of the model are consistent with experimental findings. [S1063-651X(99)05307-6]

PACS number(s): 87.10.+e, 82.20.Wt, 82.40.Bj

I. INTRODUCTION

Microtubules are tubular polymers formed from the protein tubulin. They are one of the three filament types that constitute the eukaryotic cytoskeleton and are intrinsic to many cell functions. As additional research is performed on these structures, more and more fascinating features are revealed. One of the most intriguing properties pertains to the growth characteristics of microtubules. For many years, the dynamic instability of individual microtubules has been known and studied, but another behavior is also observed. When an ensemble of microtubules has the correct buffer conditions, the total amount of assembled tubulin undergoes damped oscillations [1–4]. These oscillations are typically observed turbidimetrically. This method measures the amount of light scattering from the sample which is proportional to the amount of assembled tubulin. Since this is a bulk measurement, all of the spatial information about where assembly is taking place is eliminated, thus leaving the impression that these are simply oscillations in time, homogeneous throughout the sample. This may be the case in some situations, but other possibilities exist. Mandelkow *et al.* [5] performed an experiment where they actually viewed microtubule oscillations by eye and they observed waves in the sample. These waves of assembly were nucleated at the boundary of the vessel containing the sample and propagated inwards through the buffer.

There have been many different oscillation models developed in previous years [3,6–9]. These models varied in both their approaches and their success. Another model involving chemical kinetics [10] was shown to reproduce many of the observed microtubule oscillation phenomena. The variables in this model had no spatial dependence and the oscillations produced were purely temporal, in accordance with most experimental results. We will use this model as a starting point and make the necessary additions to include spatial dependence. The results of this model will be discussed and compared with those from experiment.

II. ADDING SPATIAL DEPENDENCE

The chemical kinetics model presented earlier [10] was based on five basic reactions involving microtubule and tubulin dimers bound with either guanosine triphosphate (GTP) or guanosine diphosphate (GDP). The set of reactions was

$$\mathrm{MT}_n + \text{Tu-GTP} \xrightarrow{k_+} \mathrm{MT}_{n+1}, \tag{1}$$

$$\mathrm{MT}_n \xrightarrow{k_c} n\,\text{Tu-GDP}, \tag{2}$$

$$n_c\,\text{Tu-GTP} \xrightarrow{k_n} \mathrm{MT}, \tag{3}$$

$$\text{Tu-GDP} \xrightarrow{k_r} \text{Tu-GTP}, \tag{4}$$

$$\mathrm{MT}_n + \text{Tu-GDP} \xrightarrow{k_i} (n+1)\,\text{Tu-GDP}, \tag{5}$$

where MT_i is a microtubule containing i dimers, and Tu-GTP/Tu-GDP is an unassembled tubulin dimer with GTP/GDP bound at the exchangeable site (E site) in the β monomer (see [10] for more details). It was assumed that all the variables depended only on time, but we will now assume space dependence as well. We also want to extend our model to include diffusion, however, not all quantities will diffuse to the same extent. Assembled microtubules are much larger than their constituent dimers and would thus diffuse much more slowly. For this reason, we will only consider the diffusion of free tubulin dimers. With these added terms, we can derive the set of reaction-diffusion equations for the above processes:

$$\dot{N} = -k_c N + k_n T_t - k_i N T_d, \tag{6}$$

$$\dot{T}_a = k_+ N T_t - k_c T_a + k_n T_t^{n_c} - k_i T_a T_d, \tag{7}$$

$$\dot{T}_d = k_c T_a - k_r T_d + k_i T_a T_d + D\nabla^2 T_d, \tag{8}$$

$$\dot{T}_t = -k_+ N T_t - n_c k_n T_t^{n_c} + k_r T_d + D\nabla^2 T_t, \tag{9}$$

where the diffusion constant D is the same for all free dimers, independent of their bound nucleotide. The four parameters are N, the microtubule number density, T_a, the density of assembled tubulin, and T_t (T_d), free tubulin dimers with GTP (GDP) bound at the E site. The rate constants for our reactions were largely determined from experimental data [10], likewise the diffusion of tubulin within the cytoplasm has been measured. Salmon *et al.* [11] found an *in vivo* value of $D = 5.9\times10^{-8}$ cm^2/s. From this they also es-

TABLE I. The constants used in the simulations (see Ref. [5] for more details).

k_+	$9\ \mu\mathrm{M}^{-1}\,\mathrm{s}^{-1}$
k_c	$0.002\ \mathrm{s}^{-1}$
k_n	$2.6\times10^{-10}\ \mu\mathrm{M}^{-2}\,\mathrm{s}^{-1}$
k_i	$0.01\ \mu\mathrm{M}^{-1}\,\mathrm{s}^{-1}$
k_r	$0.05-0.2\ \mathrm{s}^{-1}$
D	$6\times10^{-7}\ \mathrm{cm}^2/\mathrm{s}$

timated a value of $D=56\times10^{-8}$ cm^2/s for tubulin in an *in vitro* buffer. Since we are modeling *in vitro* assembly, we will adopt the second value for our choice of D. All of the constants in this model are summarized in Table I.

There has been much debate surrounding the topic of microtubule nucleation and the order of the nucleation reaction. We will select a value of $n_c=3$ in solving the above equations. Flyvbjerg *et al.* [12] used a higher order process for the initial nucleation ($n_c=6$) followed by several reactions that were third order in the monomer concentration ($n_c=3$). Although we assume complete collapse of the microtubule in reactions (2) and (5), it is more likely that some oligomers remain after collapse [13,14]. If these oligomers serve as nuclei for growth, the ensuing reactions would be third order in the dimer concentration. Although greatly simplified from the real situation, our model captures the essence of the problem and should have roughly the correct dependence on the tubulin concentration.

With all of the constants determined, we can solve the system of equations. For simplicity we will look for a solution in one spatial dimension, thus we discretize each quantity (T_a, T_d, T_t, and N) on a (x,t) grid. Because of the nonlinear terms in our equations, we selected a semi-implicit method developed by Bader and Deufhard [15]. The Laplacian was calculated using a five-point central difference formula

$$\frac{\partial^2 T_i^n}{\partial x^2} \simeq \frac{1}{3}\left[\frac{4(T_{i+1}^n-2T_i^n+T_{i-1}^n)}{\Delta x^2}-\frac{T_{i+2}^n-2T_i^n+T_{i-2}^n}{(2\Delta x)^2}\right] + O(\Delta x^4). \tag{10}$$

In this formula, the subscript i and superscript n denote the grid point (x_i,t_n) and T represents one of the reactant concentrations. We want to solve this system subject to particular boundary conditions. Since we have a closed vessel, we choose no-flux boundary conditions

$$\frac{\partial T_i^n}{\partial x}=0 \quad \text{for } i=1,N. \tag{11}$$

This can easily be incorporated into our central difference formula by artificially making each concentration profile symmetric around each boundary. Solutions to this set of reaction-diffusion equations will now be shown under a variety of conditions.

III. RESULTS OF THE MODEL

The free parameters we now have to work with are the temperature and tubulin concentration. We also have one additional freedom in that we may choose the initial conditions for the concentrations N, T_a, T_t, and T_d. If we would choose constant profiles for T_d and T_t, the diffusion terms would contribute nothing since the Laplacian would be zero and all resulting oscillations would be homogeneous in space. For nonconstant profiles, however, each part of the system will evolve based on local concentrations but would be coupled to the rest of the cell by the diffusion of the free tubulin. Systems such as this have long been known to be important in pattern formation phenomena. Turing [16] proposed reaction-diffusion models as the basis for pattern formation in chemical systems. Later models involved gradients of the concentrations to produce patterns in biological systems [17]. In any case, the basis of all pattern formation either in chemical or biological systems is the inhomogeneity of some parameter such as initial conditions, diffusion coefficients, or the rate constants. For steady-state patterns to emerge in systems with diffusion, patterns must be due to spatially inhomogeneous rate or diffusion constants since diffusion will eventually remove patterns simply due to initial conditions.

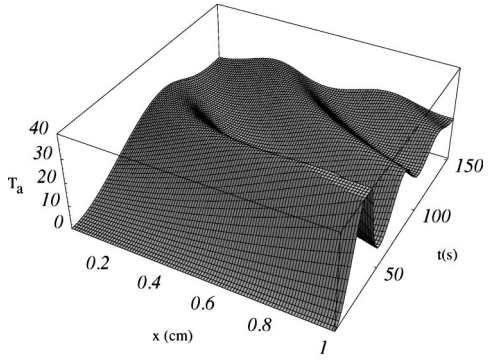

FIG. 1. Simulation for an initial gradient of Tu-GTP across the sample. The initial Tu-GTP concentration varies linearly from 50 μM at 0 cm to 100 μM at 1 cm. All other variables are initially set to zero.

In our system, the diffusion constant is very small on the scale of the other variables. Because of this, instabilities arising from diffusion are unlikely for the concentrations with which we are concerned. We know that increasing the concentration of GTP-rich tubulin increases the size of the oscillations. If we introduce an initial gradient of T_t across the cell, we would expect interesting dynamics. Figure 1 shows the results for a linear gradient of T_t from 50 μM on one edge to 100 μM on the other. Although these plots only run for a short time, it can easily be seen how initial conditions cannot produce stable patterns. At the last time step, the solution is very nearly flat. To change this result, we must assume some constant(s) to be spatially inhomogeneous.

Recall the findings of the Mandelkow group mentioned earlier. In systems where they observed waves crossing the vessel, they concluded that the barrier for nucleation was somehow lower at the boundaries. In their experiments, the buffer containing the tubulin was well mixed before the temperature jump, so we can assume homogeneous initial conditions for all variables. To try and produce such waves in our system, we adopt a nucleation rate which is highest at the edge of the cell and decays exponentially to the interior of the cell. (For simplicity, we will only raise the nucleation

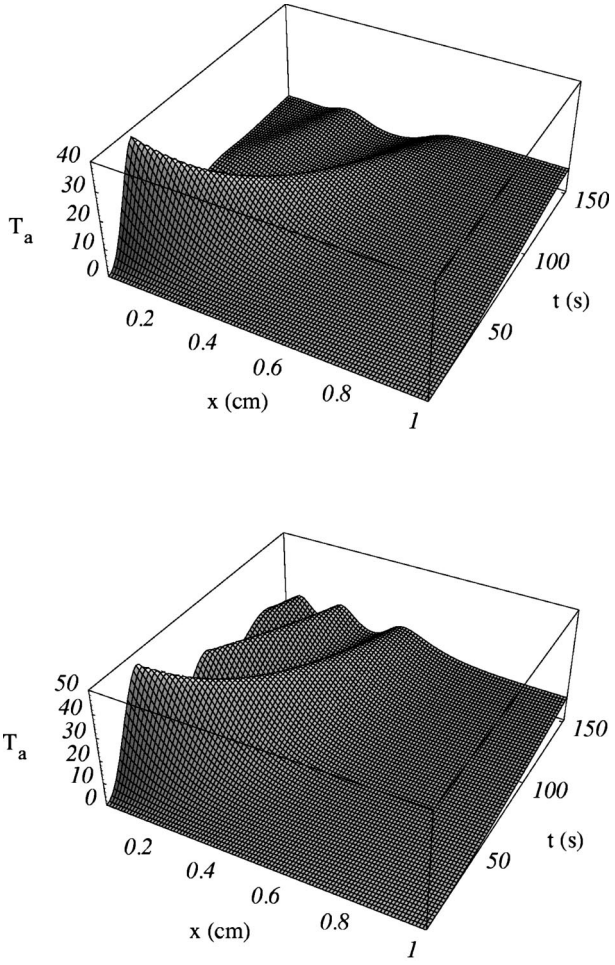

FIG. 2. Simulation for an inhomogeneous nucleation rate where k_n is highest at $x=0$ cm and falls off as $e^{-x/1\ \mathrm{cm}}$. Waves of assembled tubulin are nucleated at the boundary and propagate towards the middle of the cell. The tubulin concentration is 100 μM and k_r is equal to 0.05 s^{-1} (top) and 0.2 s^{-1} (bottom).

constant on one side of the cell.) The simulation was performed for a tubulin concentration of 100 μM where initially all of the tubulin was unassembled and GTP-rich. After nucleation at the boundary, a wave of assembled tubulin propagates into the cell center (see Fig. 2). This is in fact not a single wave, but a series of waves. As was observed by Mandelkow *et al.* [5], the waves move in from the boundary and slow as they move towards the interior of the vessel. Thus the number of visible wave crests increases with time. Figure 2 shows results for two different values of k_r. A higher value of k_r should correspond to a higher GTP concentration since it increases the rate of nucleotide exchange. In our simulations, this has the effect of increasing the size and frequency of the waves.

We can more accurately quantify the effects of the tubulin concentration and the rate of nucleotide exchange on the shape and behavior of the waves. Figure 3 shows how each of these parameters affects the average speed of the waves, the maximum wave height, and the initial separation between the first two waves. The values that we find in our model are consistent with the numbers found by Mandelkow *et al.* [5]. They reported speeds around 0.015 mm/s and wavelengths on the order of 5 mm. They also reported initial nucleation

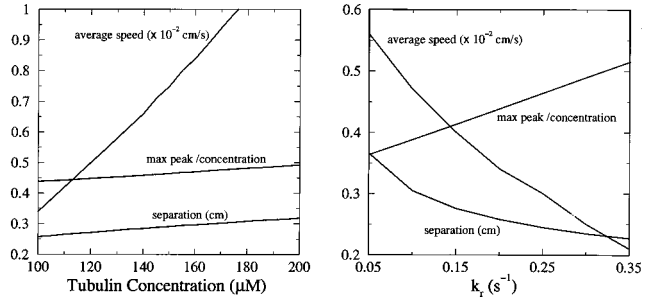

FIG. 3. The dependence of the average wave speed, the maximum peak divided by initial tubulin concentration, and the initial separation between the first and second waves as functions of initial tubulin concentration and the nucleotide exchange rate k_r. For the left plot $k_r=0.2\ s^{-1}$, for the right plot the initial tubulin concentration was 100 μM.

after about 30 s and periods of oscillations around 200 s. Again, our simulations produce values of the same order of magnitude.

As mentioned earlier, turbidimetric measurements have the effect of removing all spatial information. If we perform an average over space at each time step of our simulation, the average should correspond to the overall turbidity of the sample. Figure 4 shows three plots for different tubulin concentrations. At each concentration, there was wave formation at the boundary as depicted in the previous simulations, but at the lower concentrations, the average amount of assembly simply grew monotonically. As the tubulin concentration was increased, the plot of the average assembly developed an overshoot and eventually, with increasing concentration, oscillations.

IV. DISCUSSION

Microtubule oscillations can be produced in both time and space under the correct experimental conditions. The reaction-diffusion model presented in this paper produces qualitatively similar results. An additional feature of the model is that it draws a connection between the spatial

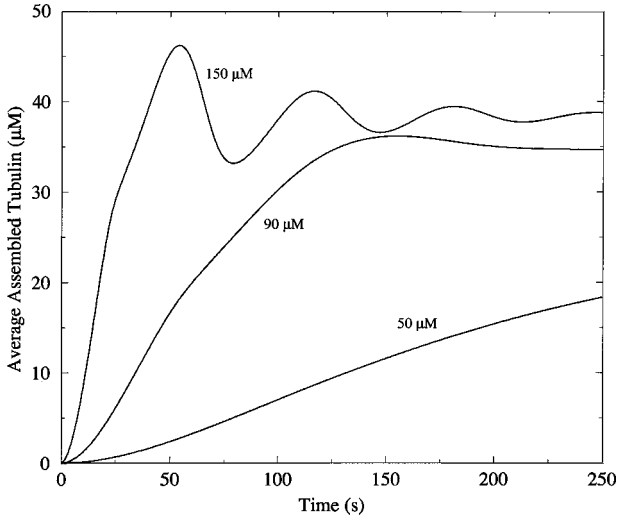

FIG. 4. The average assembled tubulin density across the sample as a function of time. The four plots are for tubulin concentrations of 50 μM (bottom), 90 μM, and 150 μM (top).

waves and turbidimetric measurements. From these results, it seems possible that waves of assembled tubulin may exist in systems where the overall turbidity of the sample does not undergo oscillations. In fact, since inhomogeneity plays such a large role in pattern formation, it would seem to be very difficult to design an experiment where homogeneous microtubule oscillations could be produced. It must be stressed that, within this model, the waves that are seen do not represent the movement of microtubules since assembled polymers are not allowed to diffuse. Instead, these waves are variations in the local stability of the growing microtubules. This is very likely the experimental situation in that these waves represent oscillations in the stability of the assembled and unassembled phases of tubulin.

The basis of this oscillation model is five simple chemical reactions along with diffusion of free tubulin dimers. There are many possibilities for extending this model to include additional effects and to make it more realistic, but we already have many degrees of freedom in the present model. The spatial dependence of the rate constants for our reactions can have a large effect. One possibility would be to choose a nucleation rate that was higher in the region of a microtubule organizing center (MTOC) and lower elsewhere. Such a choice would lead to longer microtubules in the vicinity of the MTOC and shorter ones further away. Choosing other rate constants with a spatial dependence or an inhomogeneous temperature distribution could produce many other effects.

As suggested from experimental evidence, we assumed that the nucleation rate was higher near the boundary of the vessel. The source of this increased rate is not known and may be attributed to temperature or *p*H gradients, or even dissolved gas bubbles on the sides of the vessel. For whatever reason, it is clear that the system is not completely homogeneous, and this inhomogeneity is the basis for oscillations and wave formation.

ACKNOWLEDGMENTS

The author would like to thank J. A. Tuszynski for his comments and suggestions regarding the manuscript. This work was supported by NSERC, and a NIH grant awarded to J. A. McCammon.

[1] F. Pirollet, D. Job, R.L. Margolis, and J. Garel, EMBO J. **6**, 3247 (1987).
[2] R. Melki, M.-F. Carlier, and D. Pantaloni, EMBO J. **7**, 2653 (1988).
[3] M.F. Carlier, R. Melki, D. Pantaloni, T.L. Hill, and Y. Chen, Proc. Natl. Acad. Sci. USA **84**, 5257 (1987).
[4] H. Obermann, E.-M. Mandelkow, G. Lange, and E. Mandelkow, J. Biol. Chem. **265**, 4382 (1990).
[5] E. Mandelkow, E.M. Mandelkow, H. Hotani, B. Hess, and S. Müller, Science **246**, 1291 (1989).
[6] Y. Chen and T.L. Hill, Proc. Natl. Acad. Sci. USA **84**, 8419 (1987).
[7] A. Marx and E. Mandelkow, Eur. Biophys. J. **22**, 405 (1994).
[8] B. Houchmandzadeh and M. Vallade, Phys. Rev. E **53**, 6320 (1996).
[9] E. Jobs, D.E. Wolf, and H. Flyvbjerg, Phys. Rev. E **79**, 519 (1997).
[10] D. Sept, H.J. Limbach, H. Bolterauer, and J.A. Tuszynski, J. Theor. Biol. **197**, 77 (1999).
[11] E.D. Salmon, W.M. Saxton, R.J. Leslie, M.L. Karow, and J.R. McIntosh, J. Cell Biol. **99**, 2157 (1984).
[12] H. Flyvbjerg, T.E. Holy, and S. Leibler, Phys. Rev. Lett. **73**, 2372 (1994).
[13] E.-M. Mandelkow and E. Mandelkow, J. Mol. Biol. **181**, 123 (1985).
[14] G. Lange, E.M. Mandelkow, A. Jagla, and E. Mandelkow, Eur. J. Biochem. **178**, 61 (1988).
[15] G. Bader and P. Deufhard, Numer. Math. **41**, 373 (1983).
[16] A.M. Turing, Philos. Trans. R. Soc. London, Ser. B **237**, 37 (1952).
[17] L. Wolpert, Philos. Trans. R. Soc. London, Ser. B **259**, 441 (1981).